A molecular hybrid producing simultaneously singlet oxygen and nitric oxide by single photon excitation with green light

Cristina Parisi [a,†], Mariacristina Failla [b,†], Aurore Fraix [a], Antonio Rescifina [a], Barbara Rolando [b], Loretta Lazzarato [b,*], Venera Cardile [c], Adriana C. E. Graziano [c], Roberta Fruttero [b], Alberto Gasco [b], Salvatore Sortino [a,**]

[a] Department of Drug Sciences, University of Catania, I-95125 Catania, Italy

[b] Department of Drug Science and Technology, University of Torino, I-10125 Torino, Italy

[c] Department of Biomedical and Biotechnological Sciences, Physiology Division, University of Catania, I-95125 Catania, Italy

[†] Contributed equally

Corresponding authors:

Loretta Lazzarato loretta.lazzarato@unito.it

Salvatore Sortino ssortino@unict.it

Graphical abstract

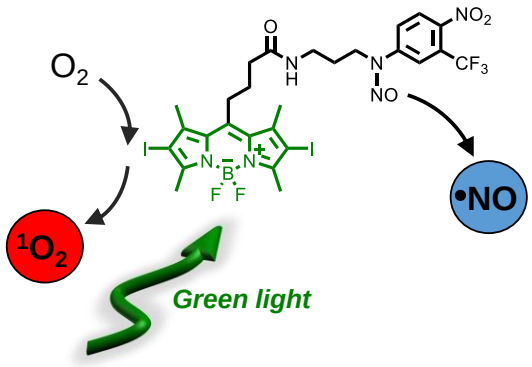

Highlights

- Singlet oxygen and nitric oxide are simultaneously generated by green light
- The molecular hybrid is not toxic in the dark towards healthy and cancer cells
- Bimodal mortality of cancer cells is observed under green light excitation

Keywords: Photodynamic therapy, Nitric oxide, Light, Multimodal therapy, BODIPY, Singlet oxygen

Abstract

Combination of photosensitizers (PS) for photodynamic therapy with NO photodonors (NOPD) is opening intriguing horizons towards new and still underexplored multimodal anticancer and antibacterial treatments not based on “conventional” drugs and entirely controlled by light stimuli. In this contribution, we report an intriguing molecular hybrid based on a BODIPY light-harvesting antenna that acts simultaneously as PS and NOPD upon single photon excitation with the highly biocompatible green light. The presented hybrid offers a combination of superior advantages with respect to the other rare cases reported to date, meeting most of the key criteria for both PSs and NOPDs in the same molecular entity such as: i) capability to generate $^1O_2$ and NO with single photon excitation of biocompatible visible light, ii) excellent $^1O_2$ quantum yield and NO quantum efficiency, iii) photogeneration of NO independent from the presence of oxygen, iv) large light harvesting properties in the green region. Furthermore, this compound together with its stable photoproduct, is well tolerated by both normal and cancer cells in the dark and exhibits bimodal photomortality of cancer cells under green light excitation due to the combined action of the cytotoxic $^1O_2$ and NO.

1. Introduction

Singlet oxygen ($^1O_2$) is the main species involved in photodynamic therapy (PDT), a well-established therapeutic modality for treating malignant lesions, including cancer, and a variety of microbial infections [1-4]. This promising treatment modality exploits the effects originated by the appropriate combination of Vis/NIR light with a photosensitizer (PS) in the presence of molecular oxygen [5]. Upon light absorption, the PS reaches its lowest-energy excited triplet state through intersystem crossing (isc). Due to the long lifetime, the triplet state can be quenched by nearby molecular oxygen mainly through energy transfer mechanisms, producing the highly reactive $^1O_2$ in a photocatalytic fashion [6, 7].

Nitric oxide (NO), is an endogenous messenger that is ubiquitously produced by mammalian tissues and is involved in many physiological and pathophysiological processes [8, 9]. Besides, NO represents an intriguing therapeutic species with exciting prospects in healthcare, including cancer, bacteria, and cardiovascular diseases [10]. In this context, the light-controlled generation of NO achieved by using suitable NO photodonors (NOPDs), has recently received a great deal of attention for use as a potential new anticancer and antibacterial agents [11-13]. Indeed, unlike classical NO-donors [14], these light-activated precursors allow the action of NO to be confined within the irradiated area with high spatial precision and its dosage, which is critical to observe therapeutic effects [15], to be controlled with great accuracy by tuning the duration and intensity of the irradiation [11-13]. In contrast to traditional PDT, the so-called NO-photodynamic therapy (NOPDT) [16] implies a net photochemical reaction to generate NO, which consumes the NOPD but, advantageously, does not require O_2 availability to function. In particular, NOPDT may be useful in the treatment of hypoxic tumors and anaerobic bacteria, which are not responsive to classical PDT [17]. In recent years, a deal of attention has been devoted to the combination of PSs and NOPD as a very appealing strategy in view of multimodal therapeutic approaches entirely controlled by light [18]. This interest is motivated by the common features that $^1O_2$ and NO share, such as small size, good lipophilicity and absence of charge, capability to be multitarget cytotoxic agents, absence of multidrug resistance, confinement of their action to short distances from the production site inside the cells due to their short lifetime in this environment (*ca.* 3 μs and *ca.* 5 s for $^1O_2$ and NO, respectively [7-9]), reducing systemic toxicity issues common to many conventional drugs. A number of supramolecular nanoconstructs assembling NOPDs and PDT PSs through appropriate carriers have been achieved in the recent years [18]. The non-covalent approach presents the advantage of the facile tuning of the relative concentrations of the photoactive guests; however, it may suffer displacement in a biological environment. In contrast, the covalent connection of the photoactive precursors within the same molecular skeleton ensures that the photodelivery events occur exactly in the "very same

region of space" of the cell components. Only a very limited number of examples of robust bifunctional systems integrating covalently PSs and NOPDs within the same molecular skeleton are known to date [19, 20]. Santana da Silva *et al.* reported an intriguing ruthenium-phthalocyanine complex having NO as axial ligand able to release NO and $^1O_2$ under light excitation [20]. However, the presence of oxygen was strictly required for the mechanism leading to NO photorelease, precluding, in principle, the advantages that NO offers under hypoxic conditions (*vide supra*). Furthermore, the efficiency of NO photorelease dropped significantly down under excitation with visible light with respect to that observed under UV light.

We recently reported the non-metal based molecular hybrid **2** (Scheme 1) in which a nitroaniline derivative NOPD was linked to a BODIPY derivative as PS [19]. These two chromogenic units represent independent light harvesting antennae in the blue and the green region of the visible spectrum, and their individual photochemical properties are conserved in the molecular conjugate. Thus, photogeneration of the cytotoxic $^1O_2$ and NO can be observed simultaneously but only under concomitant excitation with both green and less biocompatible blue light.

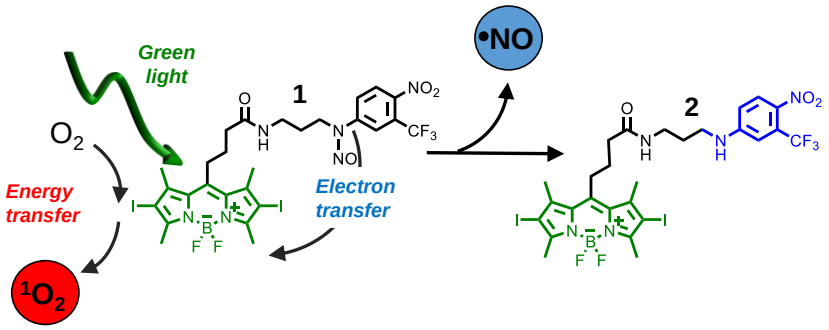

Scheme 1. Structures of the molecular hybrids **1** and **2** and working principle for the simultaneous release of $^1O_2$ and NO upon photoexcitation of **1**.

This contribution reports the novel molecular hybrid **1** that overcomes the limitations of the above systems (Scheme 1). This compound can be easily obtained in one-step by nitrosation of compound **2** (see SI) and represents the first example of molecular conjugate capable to generate simultaneously $^1O_2$ and NO exclusively upon excitation with the highly biocompatible green light. We demonstrate that these two biologically relevant species can be obtained by exploiting exclusively the BODIPY as a light-harvesting antenna. Single photoexcitation with green light triggers not only effective photogeneration of $^1O_2$ but also the release of NO from the nitrosoaniline derivative, more likely due to an intramolecular electron transfer, forming compound **2** as the main stable co-product (Scheme 1).

2. Results and Discussion

Excitation of **1** at 532 nm leads to the generation of $^1O_2$ in very high yield. In particular, $^1O_2$ was unequivocally detected and quantified by measuring its phosphorescence in the near-IR spectral window. Figure 1 shows the typical luminescence signal with maximum at ca. 1270 nm, observed for optically-matched solutions of **1** and, for comparison, of **2**. The quantum yield for production of $^1O_2$ for the conjugate **1** was $\Phi_\Delta = 0.90$, which is basically the same to that observed for **2**, suggesting that nitrosation of the nitroaniline moiety does not affect the photosensitizing properties of the BODIPY PS.

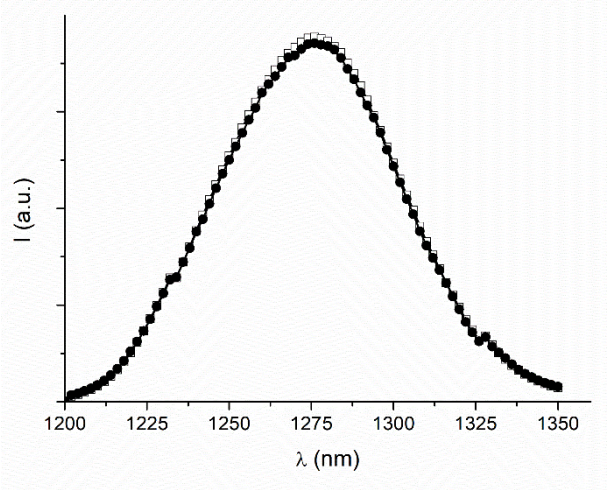

Fig. 1. $^1O_2$ luminescence detected upon 532 nm light excitation of optically matched methanol solutions of **1** (●) and **2** (□).

Figure 2A shows the absorption spectrum of **1** and, for comparison, of **2**. It can be seen that the typical absorption of the nitroaniline component at *ca.* 380 nm is much smaller in compound **1** and is accompanied by a new absorption at ca. 290 nm. This is a consequence of the loosing of the push-pull character of the nitroaniline chromophore upon nitrosation. Furthermore, the absorption band due to the BODIPY component undergoes ca. 20% hyperchromic effect that would account for an electronic interaction between the BODIPY core and the nitroso-derivative appendage (*vide infra*) in the ground state. Irradiation of a solution of **1** with green light, leads to the absorption spectral changes illustrated in Figure 2B.

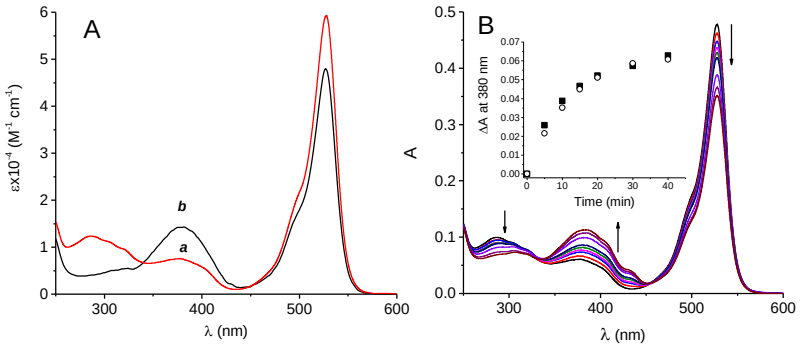

Fig. 2. (A) Absorption spectra of solutions of **1** (***a***) and, for comparison, **2** (***b***). (B) Absorption spectral changes observed upon exposure of a solution of **1** (7.5 μM) at λ_{exc} = 532 nm for intervals from 0 to 40 min. The arrows indicate the course of the spectral profile with the illumination time. The inset shows the difference absorbance changes at λ = 390 nm observed for air-equilibrated (■) and N_2-saturated (○) solutions. H_2O: MeOH (20:80 v/v). T = 25 °C.

Interestingly, a decreasing of the absorption at λ = 290 nm and λ = 527 nm and the restoring of the absorption at λ = 380 nm, typical for the nitroaniline unit of compound **2**, characterize the spectral profile evolution. These spectral changes are accompanied by the presence of two clear isosbestic points, which are indicative of the occurrence of a very clean photochemical reaction. Note that, the spectrum at the end of the photolysis is basically identical to that of compound **2** (see spectrum ***b*** in Fig. 2A). This behavior provides a first indication for the release of NO from **1** and would account for the formation of **2** as stable co-product. This hypothesis was confirmed by HPLC analysis of the irradiated reaction mixture that revealed **2** as the sole photolysis stable product (Fig. S1). Moreover, experiments carried out with N_2-saturated solutions showed that the presence of oxygen affects neither the nature nor the efficiency of the photolysis (Fig. 2B, inset and Fig. S2). This finding suggests that NO photorelease takes place independently from oxygen and rules out the participation of the long-lived excited triplet state as a key intermediate in the mechanism of the NO photorelease. The release of NO with green light was proven by the direct detection of this species through amperometric techniques using an ultrasensitive NO electrode. Figure 3 shows unambiguously that NO release by **1** takes place exclusively under light stimuli whereas stops in the dark and restarts again once the light is turned on.

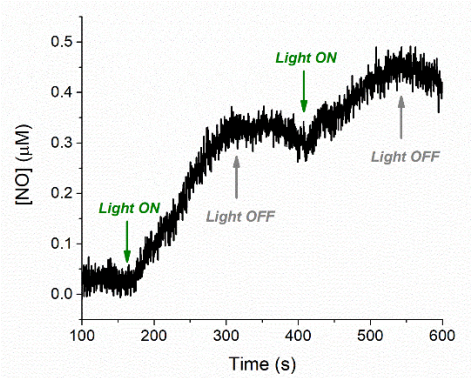

Fig. 3 NO release profile observed upon 532 nm light irradiation of a solution of **1** (7.5 μM). H_2O:MeOH (20:80 v/v). T = 25 °C.

The quantum yield for the photodecomposition of **1**, Φ_P, was 0.002 ±0.0005. This value is comparable with others organic NOPDs activatable with green light [21, 22]. Furthermore, it needs to be considered that the efficiency of photoinduced reactions is, in general, expressed as the product of $\varepsilon_{max}\Phi_P$ (quantum efficiency). In our case, the large value of ε_{max} (59.000 M^{-1} cm^{-1}) gives a product $\varepsilon_{max}\Phi_P$ ~120. Such a value is larger than the values reported for other organic NOPDs ($\varepsilon_{max}\Phi_P$ = 10−70) [23, 24] that, however, can be solely controlled with relatively toxic blue light, and is on the same order of magnitude than that recently observed of another NOPD activatable by green light [21, 22] which, however, does not produce $^1O_2$.

Since the BODIPY unit is the sole chromophore absorbing the green light, photorelease of NO from the nitro-derivative moiety must necessarily involve an electronic communication between these two components. Photoinduced energy transfer from the excited BODIPY to the nitroso-derivative appendage is, of course, out of question because it is thermodynamically uphill [25]. More likely, the uncaging of NO from **1** seems to be triggered by a photoinduced electron transfer from the nitrosoaniline-derivative moiety, as electron donor, to the excited singlet state of the BODIPY, as electron acceptor. This process encourages the detachment of NO from **1**, according to what recently observed by Nakagawa *et al.* for other BODIPYs conjugates working under blue light excitation [24], and is expected to generate a nitroaniline-derivative radical intermediate (see Scheme 2). Such a species is very stable, almost insensitive to the presence of oxygen and can evolve to the stable photoproduct **2** upon H-abstraction from solvent, in excellent agreement with the identical photolytic behavior observed in aerobic and anaerobic conditions (Figs. 2B and S2).

Our proposal is supported by a considerable change in free energy for the photoinduced electron transfer process, $\Delta G \cong -0.4$ eV estimated by the Rehm-Weller equation [26]:

$$\Delta G = e[E_{ox} - E_{red}] - E_{0,0}$$

where E_{ox} is the half-wave potential for one-electron oxidation of the electron-donor unit (*ca.* 1 eV *vs.* SCE) [27] E_{red} is the half-wave potential for one-electron reduction of the electron-acceptor unit (*ca.* –1 eV *vs.* SCE) [28, 29] and $E_{0,0}$ is the energy of the lowest excited singlet state of the BODIPY antenna (*ca*. 2.4 eV) [30]. The emissive behavior of **1** is in excellent agreement with this view. In fact, the fluorescence quantum yield of **1** was $\Phi_f = 0.044$, a value smaller than that observed for the non-nitrosate derivative **2**, $\Phi_f = 0.047$ (Fig. S3). Such a difference accounts very well for the occurrence of the photodecomposition process leading to the NO release, competitive with the fluorescence emission in the hybrid **1**. Photoinduced electron transfer between two species separated by an insulator spacer like in the case of **1**, requires, of course, their very close spatial proximity. The hyperchromic effect noted in the absorption spectrum of **1**, when compared with the non-nitrosated derivative **2** (Fig. 2A) is in line with an interaction between the electron donor and the acceptor. This is well corroborated by molecular dynamics (MD) simulation of 50 ns and the subsequent optimization of the most stable conformer at B3LYP DFT level. The obtained conformer (Fig. 4A) shows an evident U-shape like geometry in which the aromatic systems of both BODIPY and nitrosoaniline-derivative moieties are facing each other, almost in parallel, generating secondary orbital stabilizing interactions. In particular, from the results of the secondary-order perturbation theory (SOPT) analysis of the Fock matrix in NBO basis, according to the definition of delocalization energy given by Weinhold [31, 32], emerged that the U-shaped conformer is stabilized by a series of delocalizations of which the main are the $n \rightarrow \sigma^*$ (1.20 kcal/mol) between the lone pair of O_{41} and the antibonding orbital of the C_{14}–H_{52} single bond and another three $n \rightarrow \sigma^*$ (1.26, 0.83, and 0.29 kcal/mol) due to the F_{10} lone pairs with the antibonding orbital of the C_{43}–H_{72} single bond (Fig. 4B), for a total stabilization of 3.58 kcal/mol. Moreover, a hydrogen bond interaction between the amidic hydrogen atom and the oxygen atom of the *N*-nitroso moiety gives further rigidity to the distal part of the tethering trimethylene chain (2.31 kcal/mol, Fig. 4).

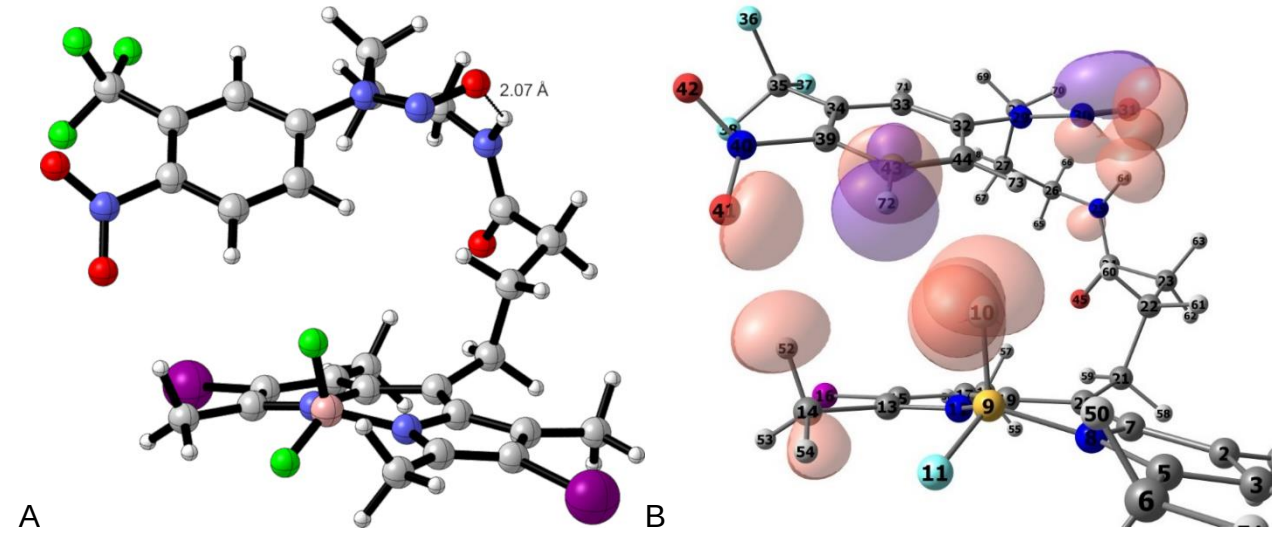

Fig. 4. A) Ball and stick representation of the most stable conformer of compound **1** in its ground state. B) Principal secondary orbital interactions of compound **1** in its most stable U-shaped conformation as derived by the SOPT analysis.

A general mechanism accounting for the photogeneration of $^1O_2$ and NO from **1** and according to the experimental results is proposed in Scheme 2.

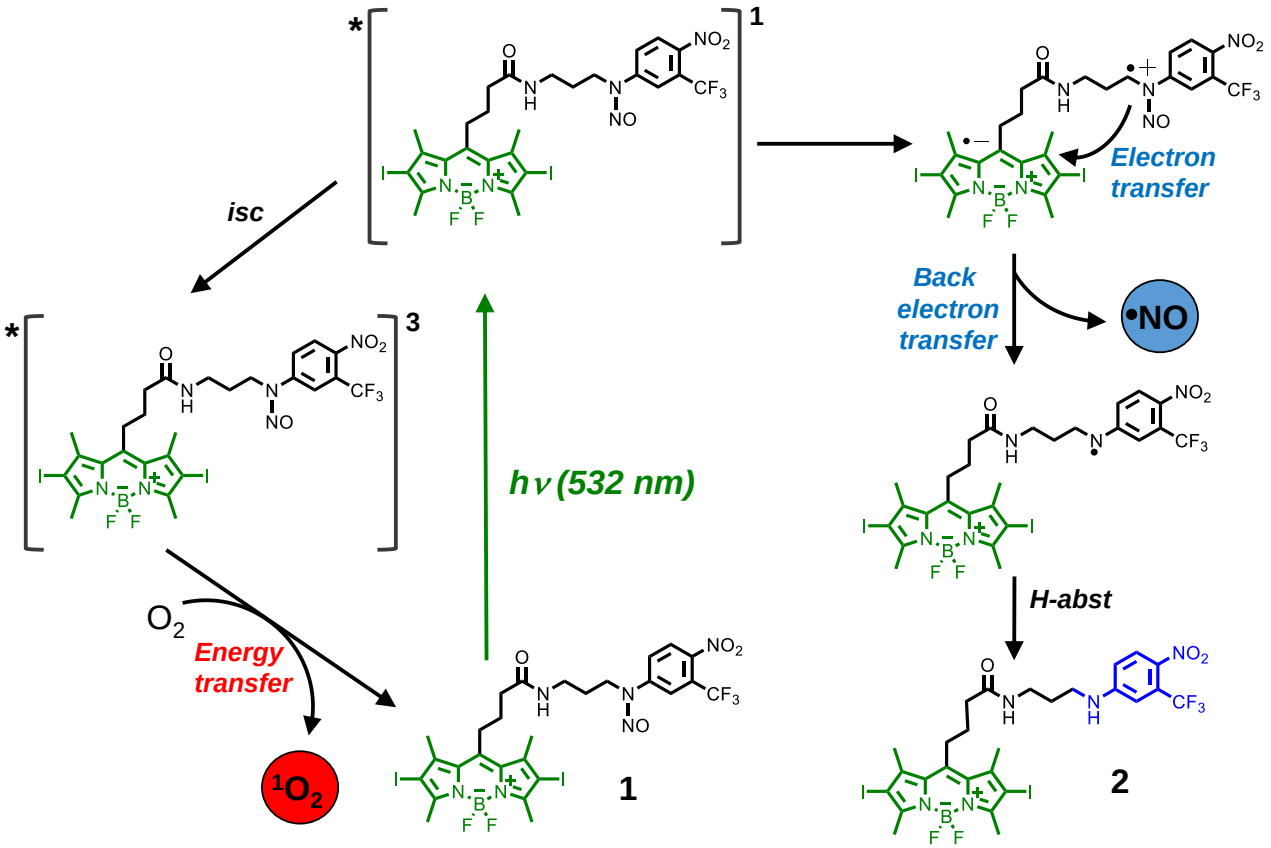

Scheme 2. General mechanism for the simultaneous release of $^1O_2$ and NO upon green light excitation of the molecular hybrid **1**.

Preliminary biological test performed to ascertain the biocompatibility of compound **1** and its stable photoproduct **2**, were carried out with human fibroblasts and A375 and HepG2 cancer cell lines. Figure S4 shows that both the molecular hybrids are well tolerated in the dark up to 10 µM by normal and tumor cells. Note that, although low, such a concentration range is enough to make **1** able to absorb considerable green light due to its large molar absorptivity (Fig. 2A). To validate the feasibility of the molecular hybrid **1** as a powerful bimodal phototherapeutic agent activatable with green light, the above cancer cell lines were incubated with **1** and, for comparison, with the same concentration of **2**, and either kept in the dark or irradiated for 5 min with a green light source. Cell cytotoxicity was determined using the MTT assay 24 h after completion of irradiation. The results in Figure 5 account for a marked cell mortality under illumination in the presence of both compounds. In particular, the extent of photomortality induced by **1**, able to photogenerate simultaneously $^1O_2$ and NO, was greater than that observed for compound **2** which, in contrast, does not produce NO under green light excitation. Such a difference being much more evident in the case of the HepG2 cancer cells. These findings provide clear-cut evidence for the involvement of a bimodal photo-inactivation mechanism in neoplastic destruction, in which the simultaneous release of cytotoxic NO and $^1O_2$ is envisaged to play a key role. At first sight, the observed bimodal action can seem surprising in view of the large difference in the photogeneration efficiency of NO and $^1O_2$ by **1**. This could be due to the different mechanism of action of these two species, according to what already proposed in the literature [20]. Mechanistic studies addressed to shed light into this issue are already ongoing in our laboratories.

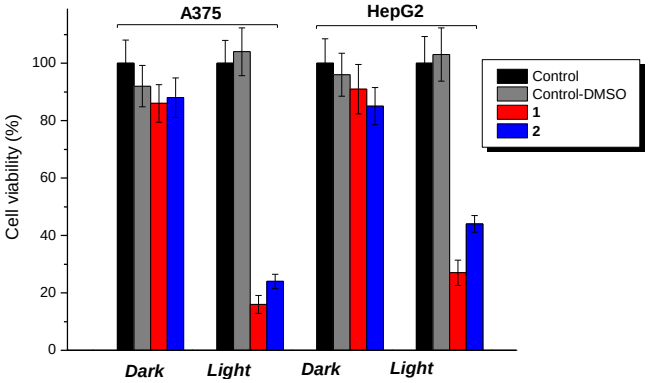

Figure 5. Cell viability of A375 and HepG2 cancer cells incubated 4h with **1** and **2** and either kept in the dark or irradiated for 5 min with green light (528 nm ≈0.5 mW cm^{-2}) [**1**] = [**2**] = 5 µM.

3. Conclusions

In conclusion, we have reported an intriguing molecular system which, to the best of our knowledge, represents the first example of a molecular hybrid offering a combination of superior advantages with respect to the other few examples reported to date. In fact, it meets most of the key criteria for both PSs and NOPDs in the same molecular entity such as: i) capability to generate $^1O_2$ and NO with single photon excitation of biocompatible green light, ii) excellent $^1O_2$ quantum yield and NO quantum efficiency, iii) photogeneration of NO independent from the presence of oxygen, iv) large light harvesting properties in the green region. Furthermore, this compound can be easily obtained in one single step from **2** and, together with its stable photoproduct, is well tolerated by both normal and cancer cells in the dark and exhibits bimodal photomortality of cancer cells under green light excitation due to the combined action of NO and $^1O_2$. These properties make **1** a very appealing candidate for a variety of forthcoming biomedical studies, especially on anticancer and antibacterial research.

Acknowledgments

We thank AIRC Project IG-19859 and Ricerca Locale from the University of Turin for financial support.

Appendix A. Supplementary data

Supplementary data related to this article can be found at https://doi.org/

References and Notes

[1] T.J. Dougherty, J.E. Kaufman, A. Goldfarb, K.R. Weishaupt, D. Boyle, A. Mittleman, Photoradiation therapy for the treatment of malignant tumors, Cancer Res., 38 (1978) 2628-2635.

[2] M.R. Hamblin, T. Hasan, Photodynamic therapy: a new antimicrobial approach to infectious disease?, Photochem. Photobiol. Sci., 3 (2004) 436-450.

[3] C.A. Robertson, D.H. Evans, H. Abraharnse, Photodynamic therapy (PDT): A short review on cellular mechanisms and cancer research applications for PDT, Journal of Photochemistry and Photobiology B-Biology, 96 (2009) 1-8.

[4] M.M. Gois, C. Kurachi, E.J.B. Santana, E.G.O. Mima, D.M.P. Spolidorio, J.E.P. Pelino, V.S. Bagnato, Susceptibility of Staphylococcus aureus to porphyrin-mediated photodynamic antimicrobial chemotherapy: an in vitro study, Lasers Med. Sci., 25 (2010) 391-395.

[5] A.P. Castano, P. Mroz, M.R. Hamblin, Photodynamic therapy and anti-tumour immunity, Nat.

Rev. Cancer, 6 (2006) 535-545.

[6] J.P. Celli, B.Q. Spring, I. Rizvi, C.L. Evans, K.S. Samkoe, S. Verma, B.W. Pogue, T. Hasan, Imaging and Photodynamic Therapy: Mechanisms, Monitoring, and Optimization, Chem. Rev., 110 (2010) 2795-2838.

[7] P.R. Ogilby, Singlet oxygen: there is indeed something new under the sun, Chem. Soc. Rev., 39 (2010) 3181-3209.

[8] L.J. Ignarro, Preface to this special journal issue on nitric oxide chemistry and biology, Arch. Pharm. Res., 32 (2009) 1099-1101.

[9] L.J. Ignarro, Editor, Nitric Oxide: Biology And Pathobiology, Second Edition, Elsevier Inc., 2010.

[10] A.W. Carpenter, M.H. Schoenfisch, Nitric oxide release: Part II. Therapeutic applications, Chem. Soc. Rev., 41 (2012) 3742-3752.

[11] S. Sortino, Light-controlled nitric oxide delivering molecular assemblies, Chem. Soc. Rev., 39 (2010) 2903-2913.

[12] N.L. Fry, P.K. Mascharak, Photoactive Ruthenium Nitrosyls as NO Donors: How To Sensitize Them toward Visible Light, Acc. Chem. Res., 44 (2011) 289-298.

[13] P.C. Ford, Photochemical delivery of nitric oxide, Nitric Oxide-Biology and Chemistry, 34 (2013) 56-64.

[14] P.G. Wang, M. Xian, X.P. Tang, X.J. Wu, Z. Wen, T.W. Cai, A.J. Janczuk, Nitric oxide donors: Chemical activities and biological applications, Chem. Rev., 102 (2002) 1091-1134.

[15] D.A. Wink, J.B. Mitchell, Chemical biology of nitric oxide: Insights into regulatory, cytotoxic, and cytoprotective mechanisms of nitric oxide, Free Radic. Biol. Med., 25 (1998) 434-456.

[16] A.D. Ostrowski, P.C. Ford, Metal complexes as photochemical nitric oxide precursors: Potential applications in the treatment of tumors, Dalton Trans., (2009) 10660-10669.

[17] C. Fowley, A.P. McHale, B. McCaughan, A. Fraix, S. Sortino, J.F. Callan, Carbon quantum dot-NO photoreleaser nanohybrids for two-photon phototherapy of hypoxic tumors, Chem. Commun. (Camb.), 51 (2015) 81-84.

[18] A. Fraix, S. Sortino, Combination of PDT photosensitizers with NO photodononors, Photochem. Photobiol. Sci., (2018).

[19] A. Fraix, M. Blangetti, S. Guglielmo, L. Lazzarato, N. Marino, V. Cardile, A.C.E. Graziano, I. Manet, R. Fruttero, A. Gasco, S. Sortino, Light-Tunable Generation of Singlet Oxygen and Nitric Oxide with a Bichromophoric Molecular Hybrid: a Bimodal Approach to Killing Cancer Cells, ChemMedChem, 11 (2016) 1371-1379.

[20] L.C.B. Ramos, M.S.P. Marchesi, D. Callejon, M.D. Baruffi, C.N. Lunardi, L.D. Slep, L.M. Bendhack, R.S. da Silva, Enhanced Antitumor Activity against Melanoma Cancer Cells by Nitric

Oxide Release and Photosensitized Generation of Singlet Oxygen from Ruthenium Complexes, Eur. J. Inorg. Chem., (2016) 3592-3597.

[21] K. Kitamura, M. Kawaguchi, N. Ieda, N. Miyata, H. Nakagawa, Visible Light-Controlled Nitric Oxide Release from Hindered Nitrobenzene Derivatives for Specific Modulation of Mitochondrial Dynamics, ACS Chem. Biol., 11 (2016) 1271-1278.

[22] M. Blangetti, A. Fraix, L. Lazzarato, E. Marini, B. Rolando, F. Sodano, R. Fruttero, A. Gasco, S. Sortino, A Nonmetal-Containing Nitric Oxide Donor Activated with Single-Photon Green Light, Chemistry-a European Journal, 23 (2017) 9026-9029.

[23] E.B. Caruso, S. Petralia, S. Conoci, S. Giuffrida, S. Sortino, Photodelivery of nitric oxide from water-soluble platinum nanoparticles, J. Am. Chem. Soc., 129 (2007) 480-481.

[24] N. Ieda, Y. Hotta, N. Miyata, K. Kimura, H. Nakagawa, Photomanipulation of Vasodilation with a Blue-Light-Controllable Nitric Oxide Releaser, J. Am. Chem. Soc., 136 (2014) 7085-7091.

[25] The excited singlet state of BODIPY lies *ca*. 1 eV below that of the nitroso-derivative unit (estimated by the end of the absorption spectra of these chromophoric units).

[26] D. Rehm, A. Weller, Kinetics of Fluorescence Quenching by Electron and H-Atom Transfer, Isr. J. Chem., 8 (1970) 259-271.

[27] H. Lund, Electroörganic preparations. III. Polarography and reduction of N-nitrosamines, Acta Chem. Scand., 11 (1957) 990-996.

[28] K. Krumova, G. Cosa, Bodipy Dyes with Tunable Redox Potentials and Functional Groups for Further Tethering: Preparation, Electrochemical, and Spectroscopic Characterization, J. Am. Chem. Soc., 132 (2010) 17560-17569.

[29] L. Huang, W.B. Yang, J.Z. Zhao, Switching of the Triplet Excited State of Styryl 2,6-Diiodo-Bodipy and Its Application in Acid-Activatable Singlet Oxygen Photosensitizing, J. Org. Chem., 79 (2014) 10240-10255.

[30] Estimated by the end of the absorption and the onset of the fluorescence emission spectra of **1**.

[31] F. Weinhold, Encyclopedia of computational chemistry, New York : J. Wiley, Chichester ;, 1998.

[32] F. Weinhold, C.R. Landis, Valency and bonding : a natural bond orbital donor-acceptor perspective, Cambridge University Press, Cambridge, UK ; New York, 2005.